REVIEW ARTICLE

Figures and figure supplements

Searching for molecular hypoxia sensors among oxygen-dependent enzymes

Li Li *et al*.

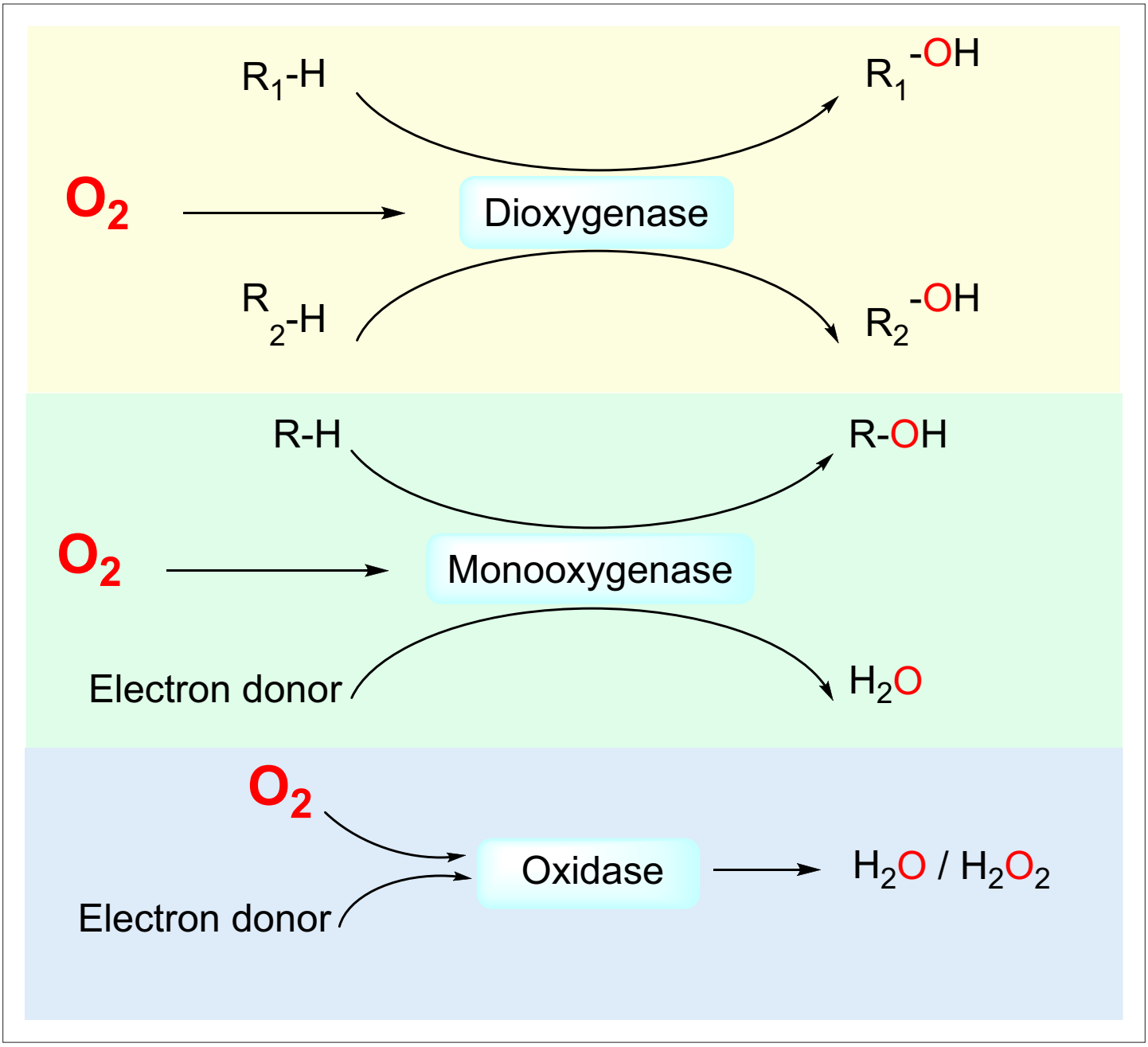

Figure 1. Three classes of by O_2-dependent enzymes (dioxygenases, monooxygenases, and oxidases) and the reactions they catalyze. Dioxygenases catalyze the insertion of both oxygen atoms of the dioxygen molecule into substrates. Monooxygenases catalyze the insertion of one oxygen atom of the dioxygen molecule into a substrate and the other oxygen atom is reduced to H_2O. Oxidases catalyze the reduction of dioxygen to H_2O or H_2O_2.

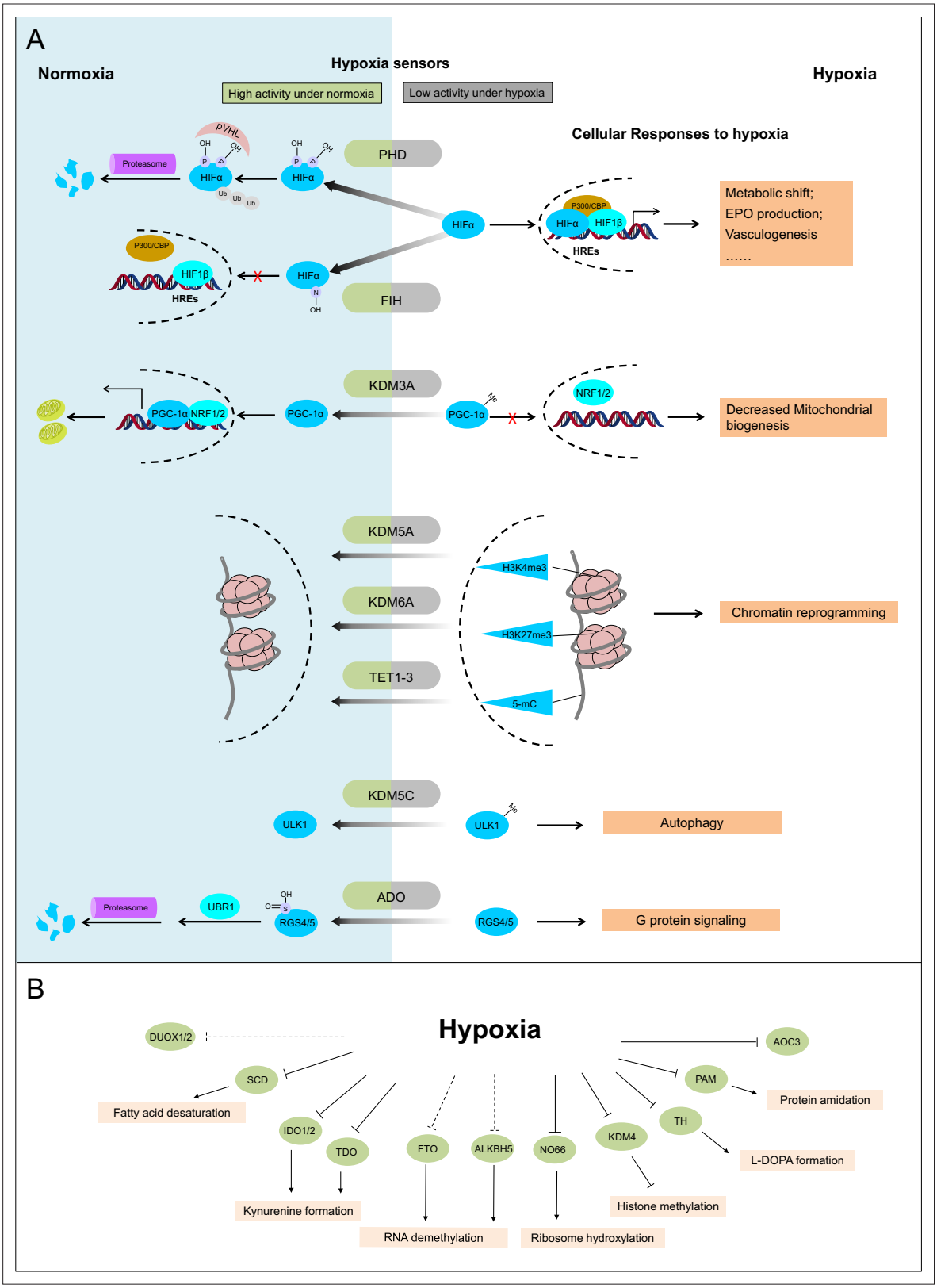

Figure 2. Known and candidate sensors for hypoxia inside O_2-dependent enzymes. (**A**) Known hypoxia sensors and their corresponding cellular responses to hypoxia. Decreased O_2 concentration inhibits activities of hypoxia sensors in O_2-dependent enzyme category and results in changes downstream signaling pathway as the cellular response to hypoxia. PHD catalyzes the hydroxylation at two prolyl residues of HIFα, and then the hydroxylated HIFα is recognized and ubiquitylated by pVHL. Following ubiquitilation, HIFα is degraded by proteasome. During hypoxia, activity of

Figure 2 continued on next page

Figure 2 continued

PHD is diminished and HIFα is stabilized. Accumulated HIFα translocates to the nucleus, and in dimerization with HIF1β, recruits other transcriptional coactivators (p300, CBP), binds with the hypoxia response elements (HREs) and activates the transcription of HIF target genes. The products of these genes participate in adaptation to hypoxia including metabolic shift, EPO production, vasculogenesis, etc. FIH catalyzes the asparaginyl hydroxylation of HIFα, and this hydroxylation inhibits HIFα from recruiting transcriptional coactivators. Compared with PHD, FIH is inhibited by more severe hypoxia. KDM3A catalyzes the demethylation of K244 monomethylation of PGC-1α, which is a transcriptional coactivator and regulates mitochondrial biogenesis. Under normoxia, PGC-1α binds with transcriptional factor NRF1/2 and activates the transcription of nucleus-encoded mitochondrial genes. Under hypoxia, the inhibited activity of KDM3A leads to accumulation of K224 monomethylation at PGC-1α. The maintained monomethylation at K224 of PGC-1α reduces its binding ability with NRF1/2 and results in decreased mitochondrial biogenesis. KDM5A catalyzes the demethylation at Lys4 of histone H3 (H3K4). Hypoxia inhibits its activity and results in the hypermethylation at H3K4, which is responsible for the gene activation. Similarly, hypoxia also inhibits KDM6A, and results in the hypermethylation at its target site H3K27 and gene repression. TET methylcytosine dioxygenases (TET1, TET2, and TET3) catalyze conversion of DNA 5-methylcytosine (5-mC) to the 5-hydroxymethylcytosine (5hmC) and mediates DNA demethylation. Hypoxia reduces TET activity and causes DNA hypermethylation. Together, these proteins sense hypoxia and lead to transcription alteration by chromatin reprogramming. KDM5C catalyzes the demethylation of ULK1 R170me2s, which regulates ULK1 activity. Under normoxia, R170me2s of ULK1 is removed by KDM5C and ULK1 remains inactive. Under hypoxia, the inhibited activity of KDM5C leads to accumulation of ULK1 R170me2s, and results in ULK1 activation and autophagy induction. ADO catalyzes the thiol oxidation at the N terminal Cys of a protein, which then triggers its degradation through N-degron pathway. Hypoxia inhibits the activity of ADO and leads to the stabilization of its substrates. One of the identified ADO substrates is RSG4/5, regulators of the G protein signaling. Stabilization of RGS4/5 results in the modulation of G-protein-coupled calcium ion signaling. (**B**) Candidate O_2 sensors with reduced enzymatic activities in hypoxia. Hypoxia leads to: inhibition of KDM4A and KDM4B and accumulated hypermethylation at H3K9; inhibition of SCD and increased cellular fatty acid saturation; inhibition of IDO and changes of immunoregulation; inhibition of PAM and reduced protein amidation; in vitro inhibition of RIOX1 and RIOX2 which are responsible for ribosome hydroxylation; in vitro inhibition of AOC3; RNA hypermethylation possibly through inhibition of FTO/ALKBH5; potential inhibition of DUOX1 and DUOX2. PHD: prolyl hydroxylase domain-containing protein; HIF: hypoxia-inducible factor; pVHL: von Hippel-Lindau protein E3 ligase; CBP, cyclic-AMP response element binding protein binding protein; EPO: erythropoietin; FIH: factor inhibiting HIF1; KDM: JmjC (Jumonji C) domain lysine demethylase; PGC: peroxisome proliferator-activated receptor gamma coactivator; NRF: nuclear respiratory factor; TET: ten-eleven translocation methylcytosine dioxygenases; ADO: cysteamine (2-aminoethanethiol) dioxygenase; RGS: regulators of G protein signalling; SCD: stearoyl-CoA desaturases; IDO: indoleamine 2,3-dioxygenase; AOC: amine oxidase, copper containing; PAM: peptidylglycine α-amidating monooxygenase; RIOX: ribosomal oxygenase, FTO: fat mass and obesity-associated protein; ALKBH: AlkB homolog; DUOX: dual oxidase.

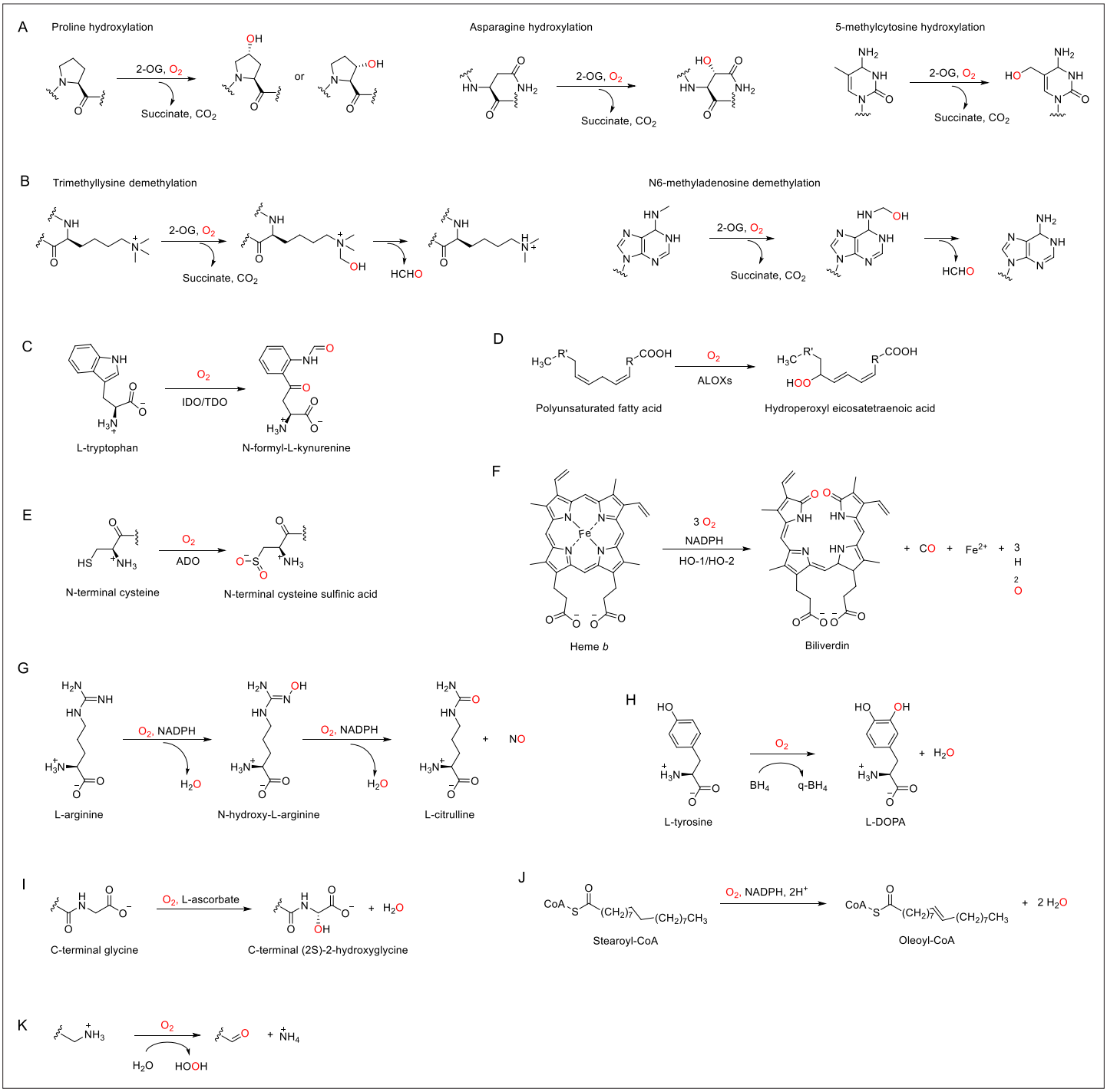

Figure 3. Enzymatic reactions catalyzed by discussed O_2-dependent enzymes. (**A**) Examples of hydroxylation reactions catalyzed by 2-OG-dependent dioxygenases. (**B**) Examples of demethylation reactions catalyzed by 2-OG-dependent dioxygenases. (**C–K**) Reactions catalyzed by indoleamine 2,3-dioxygenase (IDO)/tryptophan 2,3-dioxygenase (TDO) (**C**), arachidonate lipoxygenases (ALOXs) (**D**), (2-aminoethanethiol) dioxygenase (ADO) (**E**), heme oxygenases (HOs) (**F**), nitric oxide synthases (NOSs) (**G**), tyrosine 3-hydroxylase (TH) (**H**), peptidylglycine α-amidating monooxygenase (PAM) (**I**), stearoyl-CoA desaturase 1 (SCD1), (**J**) and copper amine oxidases (CAOs) (**K**).

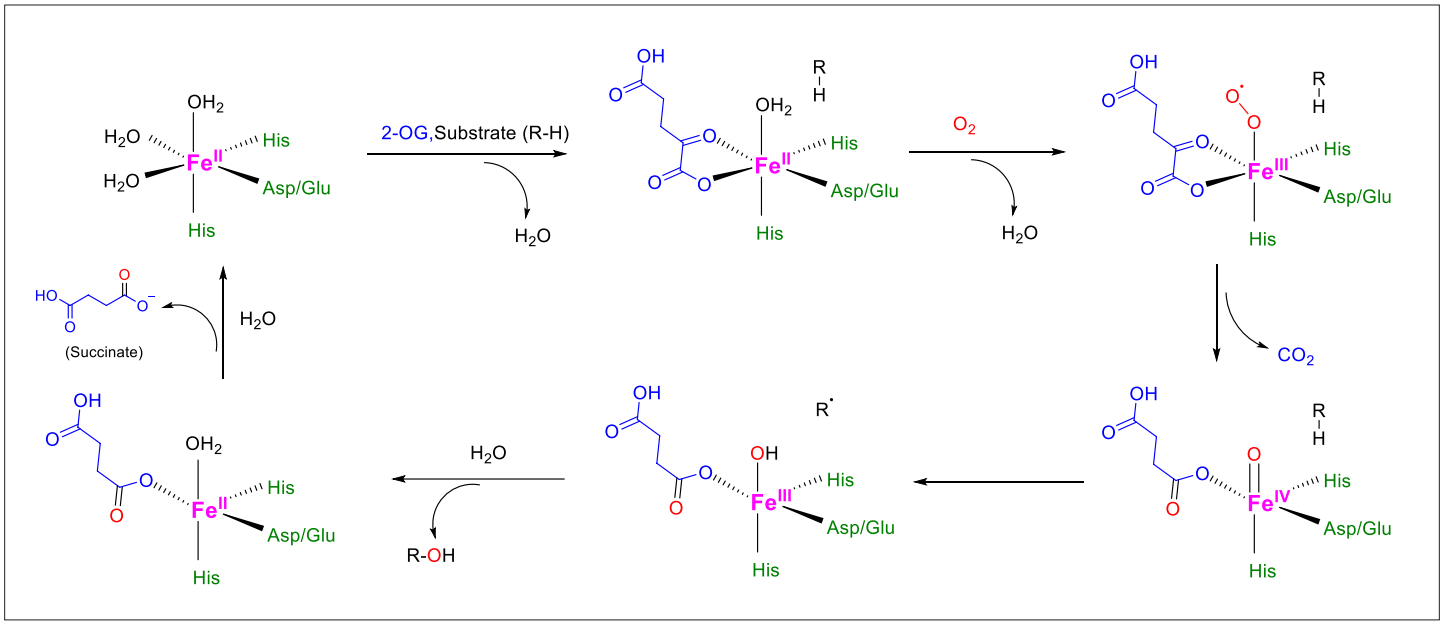

Figure 3—figure supplement 1. Catalytic mechanism for 2-OG-dependent dioxygenases. 2-OG-dependent dioxygenases share consensus mechanisms for the catalyzed hydroxylation (***Islam et al., 2018***; ***Fletcher and Coleman, 2020***; ***Rose et al., 2011***): the Fe(II) at the catalytic center is initially coordinated by 2 His side chains and a carboxylate from Glu or Asp, plus three additional H_2O molecules to complete the octahedral coordination geometry. Then, bidentate coordination of 2-OG to Fe(II) replaces 2 H_2O molecules, and the third Fe(II)-bound H_2O molecule leaves after the binding of the primary substrate into the active site, making a vacant coordination site for O_2. After the binding and activation of O_2 at the Fe(II) center, one of the O_2 atoms inserts into the primary substrate for hydroxylation, while the other O_2 atom facilitates the oxidative decarboxylation of 2-OG, forming succinate and CO_2 as co-products.

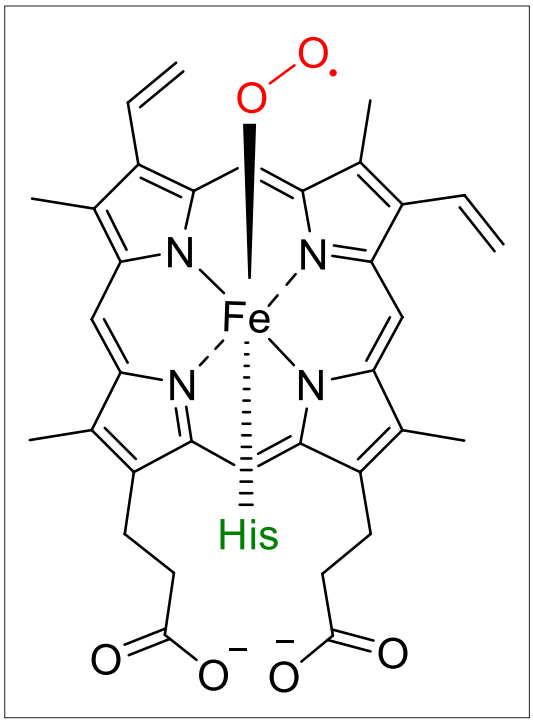

Figure 3—figure supplement 2. O_2-binding sites for dioxygenases using heme. The heme Fe(II) is coordinated by the four N atoms from the porphyrin and one N atom from one histidyl residue in the catalytic pocket, leaving the vacant coordination site for O_2 binding and activation (***Singleton et al., 2014***).

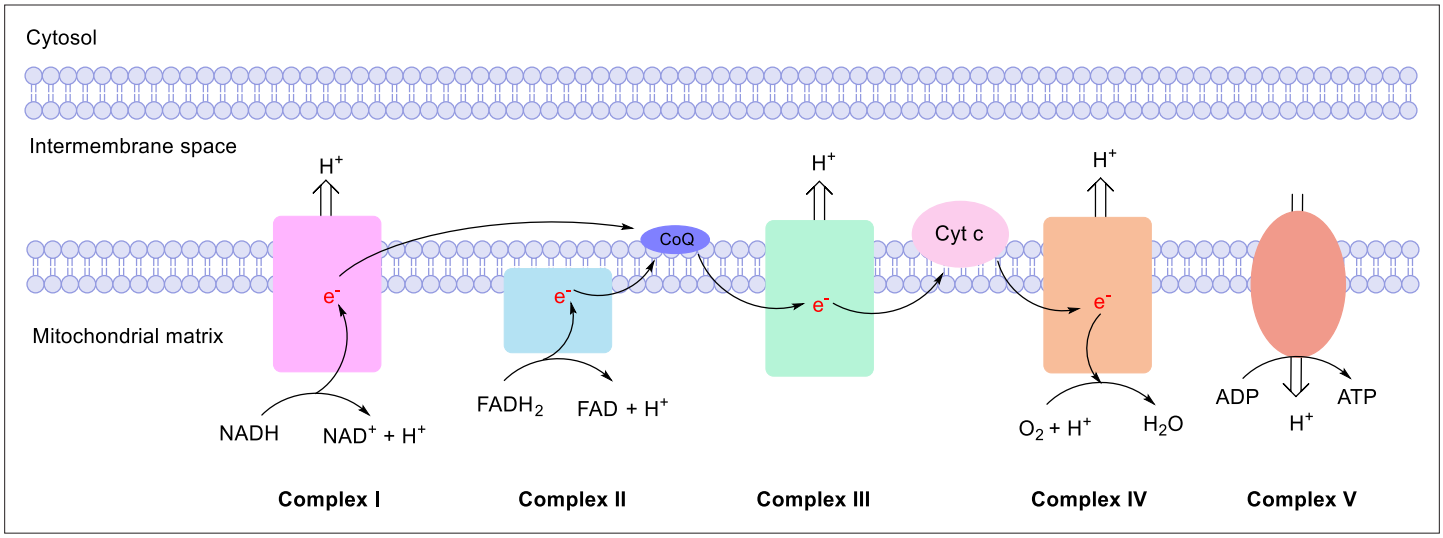

Figure 3—figure supplement 3. Mitochondrial electron transport chain (ETC). The ETC consists of NADH ubiquinone oxireductase (Complex I), succinate dehydrogenase (Complex II), $CoQH_2$-cytochrome c reductase (Complex III), and cytochrome *c* oxidase (Complex IV). In the ETC, electrons are transported from the NADH or $FADH_2$ to ubiquinone at Complex I or II, then to cytochrome *c* at Complex III, and finally to O_2 at Complex IV. This process is coupled with ATP generation at ATP synthase (Complex V) to form the oxidative phosphorylation (OxPhos) process, which is the major source of energy production.